UNCLASSIFIED

Copy No. 3

RM No. L7A03

[redacted]

NACA

RESEARCH MEMORANDUM

FORCE AND LONGITUDINAL CONTROL CHARACTERISTICS OF A 1/16-SCALE MODEL OF THE BELL XS-1 TRANSONIC RESEARCH AIRPLANE AT HIGH MACH NUMBERS

By

Axel T. Mattson

Langley Memorial Aeronautical Laboratory
Langley Field, Va.

NATIONAL ADVISORY COMMITTEE FOR AERONAUTICS

WASHINGTON

May 21, 1947

[redacted]

UNCLASSIFIED

NATIONAL ADVISORY COMMITTEE FOR AERONAUTICS

RESEARCH MEMORANDUM

FORCE AND LONGITUDINAL CONTROL CHARACTERISTICS OF A 1/16-SCALE MODEL OF THE BELL XS-1 TRANSONIC RESEARCH AIRPLANE AT HIGH MACH NUMBERS

By Axel T. Mattson

SUMMARY

This report contains a part of the results obtained to determine the effects of compressibility at high Mach numbers on a 1/16-scale model of the Bell XS-1 transonic research airplane.

Although these results do not present completely the force and longitudinal control characteristics of the model, general trends are illustrated which can at least be qualitatively analyzed for level-flight Mach numbers up to 0.93.

A large increase in drag coefficient occurs beyond a Mach number of 0.78. At a lift coefficient of 0.1 and a Mach number of 0.9, the drag coefficient has increased to approximately three times the subcritical value. At a Mach number of approximately 0.825, an initial lift force break occurs. This force break, up to a Mach number of approximately 0.875, is not severe, although elevator-control effectiveness is decreasing. At a Mach number of 0.9, however, the airplane, because of an indicated diving tendency with loss and reversal in elevator control, will require the use of the stabilizer as a trim control. Control by the use of the stabilizer is effective, at least up to a Mach number of 0.93, the limit for these tests. These results, as have the wing-flow test results, have indicated that although an airplane of a similar configuration can be controlled in level flight at transonic speed with the use of the stabilizer, a rapid and accurate manipulation of the stabilizer may be required at Mach numbers of approximately 0.90.

INTRODUCTION

At the request of the Air Materiel Command, Army Air Forces, tests were conducted in the Langley 8-foot high-speed tunnel for the purpose

[redacted]

of investigating the performance, stability, and control characteristics of the Bell XS-1 transonic research airplane. This airplane is designed to fly through the transonic region to obtain flight research information.

In order to aid in performance predictions, lift and drag polars were obtained for the basic model configuration without the simulation of rocket power. The investigation included stabilizer and elevator-effectiveness tests; however, because of incomplete tare evaluation, the pitching-moment data are presented for angles of attack of only 0° and 6°.

This report presents data which are corrected for tares. Other data, which are not presented but which have been obtained, require additional tunnel testing to evaluate the tares. By the use of the data in this report, trends in lift and drag forces and longitudinal control characteristics are indicated which may be of interest in connection with flight testing.

SYMBOLS

The symbols used in this report and their definitions are as follows:

V free-stream velocity, feet per second

ρ free-stream density, slugs per cubic foot

q dynamic pressure, pounds per square foot $\left(\frac{1}{2}\rho V^2\right)$

a velocity of sound, feet per second ($49.0\sqrt{T}$, T in $^{\circ}$F absolute)

M Mach number $\left(\frac{V}{a}\right)$

L lift, pounds

D drag, pounds

$M_{c.g.}$ pitching moment, about center of gravity (25 percent $\bar{c}$), foot-pounds

S_w wing area, 0.508 square foot

$\bar{c}$ mean aerodynamic chord, 3.607 inches, 0.3006 foot

$$C_L = \frac{L}{qS_w}$$

$$C_D = \frac{D}{qS_w}$$

$$C_{m_{c.g.}} = \frac{M_{c.g.}}{qS_w\bar{c}}$$

α angle of attack measured with respect to fuselage center line, degrees

i_t angle of incidence of the horizontal tail with respect to fuselage center line, degrees

δ_e elevator angle with respect to horizontal tail chord line, degrees

AIRPLANE AND APPARATUS

The Bell XS-1 is a research airplane designed for extreme variations in speed, wing loading, and altitude. The airplane employs a rocket motor and is equipped with an adjustable power-driven stabilizer.

For this investigation the Bell Aircraft Corporation supplied a 1/16-scale, all-metal, solid-construction model, which consisted of a wing, fuselage, and empennage. The model stabilizer could be set for incidences of $\pm 6^\circ$, $\pm 3^\circ$, and 0°. There were no gaps between the stabilizer and elevators. The three-view drawing (fig. 1) shows the principal dimensions of the model as tested in the Langley 8-foot high-speed tunnel. The physical characteristics of the XS-1 research airplane are given in table I.

The Langley 8-foot high-speed tunnel, in which this investigation was conducted, is a single-return closed-throat type capable of obtaining – tunnel empty – a Mach number of unity in the test section. The tunnel air velocity is continuously controllable. For this investigation, Mach numbers up to 0.93 were obtained by the use of a sting-support system.

Tunnel sting-support system.– In order to dispense with the interference effects of conventional support struts at high Mach numbers and to permit model testing at a Mach number approaching unity, the model was mounted on a sting-support system, as shown in figure 2. The system is characterized by a support extending from the rear of the fuselage to a shielded strut, which is connected to the tunnel balance system. A tunnel-wall liner was installed in the test section to produce a higher velocity at the model than at the strut and thus prevent the maximum Mach number from being limited by choking at the strut. Figure 3 shows the sting-support system, liner, and tare setup in the Langley 8-foot high-speed-tunnel test section.

Tare setup and evaluation.- Auxiliary arms to support the model as shown in figure 3 were used to determine the tare values of the support system and interference effects. The supports in the region of the model were 6-percent-thick airfoils swept back 30° to minimize interference effects and delay effects due to compressibility for the test Mach number range. The remaining parts of the tare supports were thin plates extending back and connected to the support strut.

The tare setups and the method by which all the data presented in this report have been corrected are illustrated in figure 4. Guy wires from the wing tips were used on all tare runs so that this system would be rigid when no sting was used. Two model tare configurations are required to evaluate the tare forces. For the tare configuration without the sting, the sting was replaced by a small fuselage fairing. (See fig. 2.) This fairing was relatively blunt because of the geometry of the fuselage contours, and also, it was felt that a longer fuselage fairing would change the basic pitching-moment characteristics of the fuselage. The assumptions included in the tare evaluation are that the interference effects of arms on sting and sting on arms are negligible.

TESTS AND MEASUREMENTS

Test Conditions

These tests were run through a Mach number range from 0.4 to approximately 0.945. The model Reynolds number ranged for these tests from approximately 1.03×10^6 to 1.18×10^6 and was based on a model mean aerodynamic chord of 3.607 inches.

Measurements

The force measurements are presented as standard NACA non-dimensional coefficients. These coefficients are based on a model wing area of 0.508 square foot. The pitching moments are taken about a center-of-gravity position (0.25 $\bar{c}$) indicated in figure 1, which also gives the principal dimensions of the model as tested in the Langley 8-foot high-speed tunnel. Each model configuration was tested through an angle-of-attack range including -4°, -2°, 0°, 2°, 4°, 6°, and 8° for Mach numbers of 0.4, 0.6, 0.7, 0.725, 0.75, 0.775, 0.8, 0.825, 0.85, 0.875, 0.9, and limited to approximately 0.945. The model configurations tested are as follows:

(a) Complete model less horizontal tail

(b) Complete model; $i_t = 0^{\circ}$, $\delta_e = -9^{\circ}$

$i_t = 0^{\circ}$, $\delta_e = -6^{\circ}$

$i_t = 0^{\circ}$, $\delta_e = -3^{\circ}$

$i_t = 0^{\circ}$, $\delta_e = 0^{\circ}$

$i_t = 0^{\circ}$, $\delta_e = 3^{\circ}$

$i_t = 0^{\circ}$, $\delta_e = 6^{\circ}$

(c) Complete model; $i_t = -6^{\circ}$, $\delta_e = 0^{\circ}$

$i_t = -3^{\circ}$, $\delta_e = 0^{\circ}$

$i_t = 3^{\circ}$, $\delta_e = 0^{\circ}$

$i_t = 6^{\circ}$, $\delta_e = 0^{\circ}$

CORRECTIONS

Because of the relatively small model required for testing at high Mach numbers, wind-tunnel corrections such as model constriction and wake constriction are small up to the highest test Mach number attained. An estimation of the tunnel correction, obtained by using methods described in references 1, 2, 3, and 4, indicates that the corrections to the Mach number will be approximately 1.5 percent at a tunnel Mach number of 0.9 for the highest lift coefficients attained. Corrections in dynamic pressure will be of the same order of magnitude. The lift vortex interference correction is small, being a change in angle of attack of less than 0.1° at the highest lift coefficient obtained. Because of the small magnitude of the corrections, they have not been applied to the data presented here.

Tunnel-wall pressure measurements showed that the flow in the test section was free of interference from tunnel choking effects and from the field of flow of the support strut at the highest Mach numbers for which data are presented.

The model was accurately constructed. The model being of all-metal construction remained the same throughout the investigation. Displacement of the model center of gravity relative to the trunnion axis of the tunnel due to air loads was continuously observed by the use of a cathetometer. Corrections for model displacements have been applied to the pitching moments. The angle of attack of the model was also checked by the use of the cathetometer; for the maximum loads obtained the change in angle of attack due to deflection of the model was of the order of 0.2 of a degree. In the angle-of-attack range from 0° to 4°, the deflections are considered negligible.

RESULTS AND DISCUSSION

Force Characteristics

Drag characteristics.- Model drag coefficients and angle of attack are presented in figure 5 as functions of lift coefficient for Mach numbers from 0.6 to 0.90. Model drag coefficients as functions of Mach number for lift coefficients of 0.1 and 0.40 are presented in figure 6. At a Mach number of 0.6 the model drag coefficient is 0.0265 for a lift coefficient of 0.1. With increasing Mach number a gradual decrease in drag coefficient occurs up to a Mach number of 0.775. This drag coefficient (that is, $C_D = 0.0265$; $M = 0.6$) and the subcritical drag-coefficient variation may be the result of the low Reynolds number for these tests. These drag results are obtained for a model with a blunt tail fairing and do not represent a jet configuration. At a Mach number of 0.78 for a lift coefficient of 0.1 a drag force break accompanied by a rapid increase in drag coefficient occurs. At a Mach number of 0.90 the drag coefficient has increased to approximately 0.071, about three times the subcritical value.

Lift characteristics.- The variation of model lift coefficient for constant angles of attack is presented against Mach number in figure 7. At an angle of attack of 0° the lift force break occurs at a Mach number of 0.80. For this condition the model lift coefficient is 0.30. With increase of Mach number to 0.875 the lift coefficient decreases rapidly to approximately 0.025. With a further increase in Mach number to 0.925 the lift coefficient increases to a value of 0.2. This increase in lift coefficient at high supercritical Mach numbers, although subject to more fundamental investigation, is believed to be mainly the result of the rearward movement of the shock disturbance on the upper surface of the wing. The formation of shock on the lower surface of the wing at low lift coefficients will tend to retard this rather rapid lift-coefficient increase. However, at the higher lift coefficients or an angle of attack of approximately 8°, the high-speed lift coefficient is well above the low-speed value.

Pitching-moment characteristics.- Figure 7 also presents the variation of the model pitching-moment coefficient with Mach number for angles of attack of 0° and 6°. Unfortunately, pitching-moment coefficients for all the angles of attack cannot be presented, as additional testing is required. However, for an angle of attack of 0° the model pitching-moment-coefficient variation with Mach number is not severe until a Mach number of 0.875 is attained. With further increase in Mach number to 0.93 a rapid increase in diving moment occurs. Although the pitching-moment coefficients are not available for other angles of attack, these results, at least qualitatively, indicate that above a Mach number of 0.875 the airplane will encounter stability and trim changes. It should be noted here that these changes in longitudinal-force characteristics occur with relatively small increases in Mach number, and control in this transonic region may require rapid manipulation of the control system.

Control characteristics.- The variation of model pitching-moment coefficient with Mach number for various elevator deflections is presented in figure 8 for a stabilizer angle of 0°. The model pitching-moment coefficients against Mach number are presented in figure 9 for an elevator deflection of 0° and various stabilizer angles. The results for the model without the horizontal tail are also presented. These results are presented for only zero angle of attack. From these figures, increments in pitching moments produced by stabilizer and elevator control are obtained by taking the difference in pitching moments between the no-deflection tail configuration ($i_t = 0^\circ$, $\delta_e = 0^\circ$) and the stabilizer and elevator-deflection configurations. These incremental pitching-moment variations with Mach number are presented in figures 10 and 11. These figures illustrate the ability of the stabilizer and elevator to produce longitudinal control.

For a Mach number range from 0.4 to approximately 0.82, figure 10 indicates that satisfactory control characteristics can be obtained for elevator deflections of ±3°. However, with increase in the elevator deflections to 6° and 9°, control effectiveness decreased through the Mach number range from 0.4 to 0.82. From a Mach number of 0.82 to a Mach number of 0.925 a large decrease in elevator effectiveness occurs. For example, at a Mach number of 0.9 the elevator as a control in deflecting from -3° to 3° is 45 percent as effective in producing changes in longitudinal pitching moments as it was at a Mach number of 0.4. It is also indicated that at a Mach number of 0.925 and at larger deflections a reversal in elevator-control effectiveness occurs.

At a Mach number of 0.9 the stabilizer-control effectiveness (fig. 11) has decreased to approximately 33 percent of its value at a Mach number of 0.4 for a range of angle of incidence from -3° to 3°. However, there is no indication (as there was with the elevator) that reversal of control effectiveness will be obtained up to stabilizer incidence angles of $\pm 6^{\circ}$.

Comparison of Results with Wing-Flow Investigation

A comparison of the results presented herein with the results obtained on a similar model configuration by the wing-flow method (reference 5) substantiates the general trends due to compressibility effects. Some quantitative differences in the comparison can be expected because of the following reasons:

(a) Reynolds number

(b) Model configuration

(c) Testing techniques

The Reynolds number for the wing-flow tests ranged from 0.32×10^6 at a Mach number of 0.6 to 0.52×10^6 at a Mach number of 0.9 as compared with 1.03×10^6 and 1.18×10^6 for the Langley 8-foot high-speed-tunnel tests. The wing-flow model, although having a fuselage similar to that of the present investigation, had a relatively larger wing and tail and also a center-of-gravity location at 27 percent of the mean aerodynamic chord as compared with 25 percent for the Langley 8-foot high-speed-tunnel model. The wing-flow tests were of a partial-span model whereas the present investigation was of a complete model configuration.

<u>General lift characteristics</u>.- The lift characteristics in the form of lift-curve slope and angle of zero lift are presented in figure 12 against Mach number. The changes in lift-curve slope for the two model configurations occur at approximately the same Mach number. For example, the Langley 8-foot high-speed-tunnel results

show that an initial decrease in lift-curve slope occurs at a Mach number of 0.78; similarly, a decrease in lift-curve slope occurs at a Mach number of 0.76 for the wing-flow results. The lift-curve slope continues to decrease to a Mach number of 0.88 for the Langley 8-foot high-speed-tunnel investigation and to a Mach number of 0.92 for the wing-flow investigation. Above these Mach numbers, an increase in lift-curve slope occurs; the Langley 8-foot high-speed-tunnel results, however, indicate a sharper increase.

The variations of angle of zero lift with Mach number obtained from both investigations show excellent agreement. (See fig. 12.) At approximately a Mach number of 0.825, a decrease (in absolute value) in angle for zero lift occurs up to approximately a Mach number of 0.89; then the angle for zero lift increases with a further increase in Mach number until, as indicated by the wing-flow results, a Mach number of 0.95 is reached.

Control-surface characteristics.- A more practical consideration is the variation of control-surface deflections required for trim with Mach number. The variations of stabilizer and elevator angles with Mach number for trim at constant angles of attack are presented in figure 13. Both investigations indicate that at Mach numbers from 0.85 to 0.93 abrupt changes occur in stabilizer and elevator angles required for trim. These trim changes may necessitate a rapid manipulation of the control surface as was previously mentioned in the discussion of pitching-moment characteristics. The present investigation also shows that the model can be trimmed at two elevator deflections as a result of reversal of elevator effectiveness.

CONCLUDING REMARKS

Although these results do not present completely the force and longitudinal control characteristics of the model, general trends are illustrated which can at least be qualitatively analyzed for level-flight Mach numbers up to 0.93. A large increase in drag coefficient occurs beyond a Mach number of 0.78. At a lift coefficient of 0.1 and and a Mach number of 0.9, the drag coefficient has increased to approximately three times the subcritical value. At a Mach number of approximately 0.825 an initial lift force break occurs. This force break, up to a Mach number of approximately 0.875, is not severe although elevator-control effectiveness is decreasing. At a Mach number of 0.9, however, the airplane, because of an indicated diving tendency with loss and reversal in elevator control, will require the use of the stabilizer as a trim control. Control by the use of the stabilizer is effective at least up to a Mach number of 0.93, the limit for these tests. These results, as have the wing-flow-test results, have indicated that, although an airplane of similar configuration can be controlled in level flight at transonic speeds with the use of the stabilizer, a rapid and accurate manipulation of the stabilizer may be required at Mach numbers of approximately 0.90.

Langley Memorial Aeronautical Laboratory
National Advisory Committee for Aeronautics
Langley Field, Va.

REFERENCES

1. Byrne, Robert W.: Experimental Constriction Effects in High-Speed Wind Tunnels. NACA ACR No. L4L07a, 1944.

2. Glauert, H.: Wind Tunnel Interference on Wings, Bodies and Airscrews. R. & M. No. 1566, British A. R. C., 1933.

3. Thom, A.: Blockage Corrections in a Closed High-Speed Tunnel. R. & M. No. 2033, British A.R.C., 1943.

4. Goldstein, S., and Young, A. D.: The Linear Perturbation Theory of Compressible Flow, with Applications to Wind-Tunnel Interference. R. & M. No. 1909, British A.R.C., 1943.

5. Zalovcik, John A., and Sawyer, Richard H.: Longitudinal Stability and Control Characteristics of a Semispan Airplane Model at Transonic Speeds from Tests by the NACA Wing-Flow Method. NACA ACR No. L6E15, 1946.

TABLE I.– PHYSICAL CHARACTERISTICS OF THE

BELL XS-1 TRANSONIC RESEARCH AIRPLANE

Power:

Four rocket units each capable of delivering 1500 pounds thrust, grouped in rear of fuselage.

Wing loading:	
Take-off, lb/sp ft	103
Landing, lb/sq ft	40
Center-of-gravity position, percent M.A.C.	25
Wing:	
Area, sq ft	130
Span, ft	28
Mean aerodynamic chord, in	57.71
Aspect ratio	6
Root and tip sections	65_1-110 (a = 1.0)
Incidence (root chord to thrust line), deg	2.5
Incidence (tip chord to thrust line), deg	1.5
Horizontal tail:	
Total area, sq ft	26.0
Span, ft	11.4
Aspect ratio	5
Root-mean-square chord of elevator, ft	0.464

NATIONAL ADVISORY
COMMITTEE FOR AERONAUTICS

[redacted]

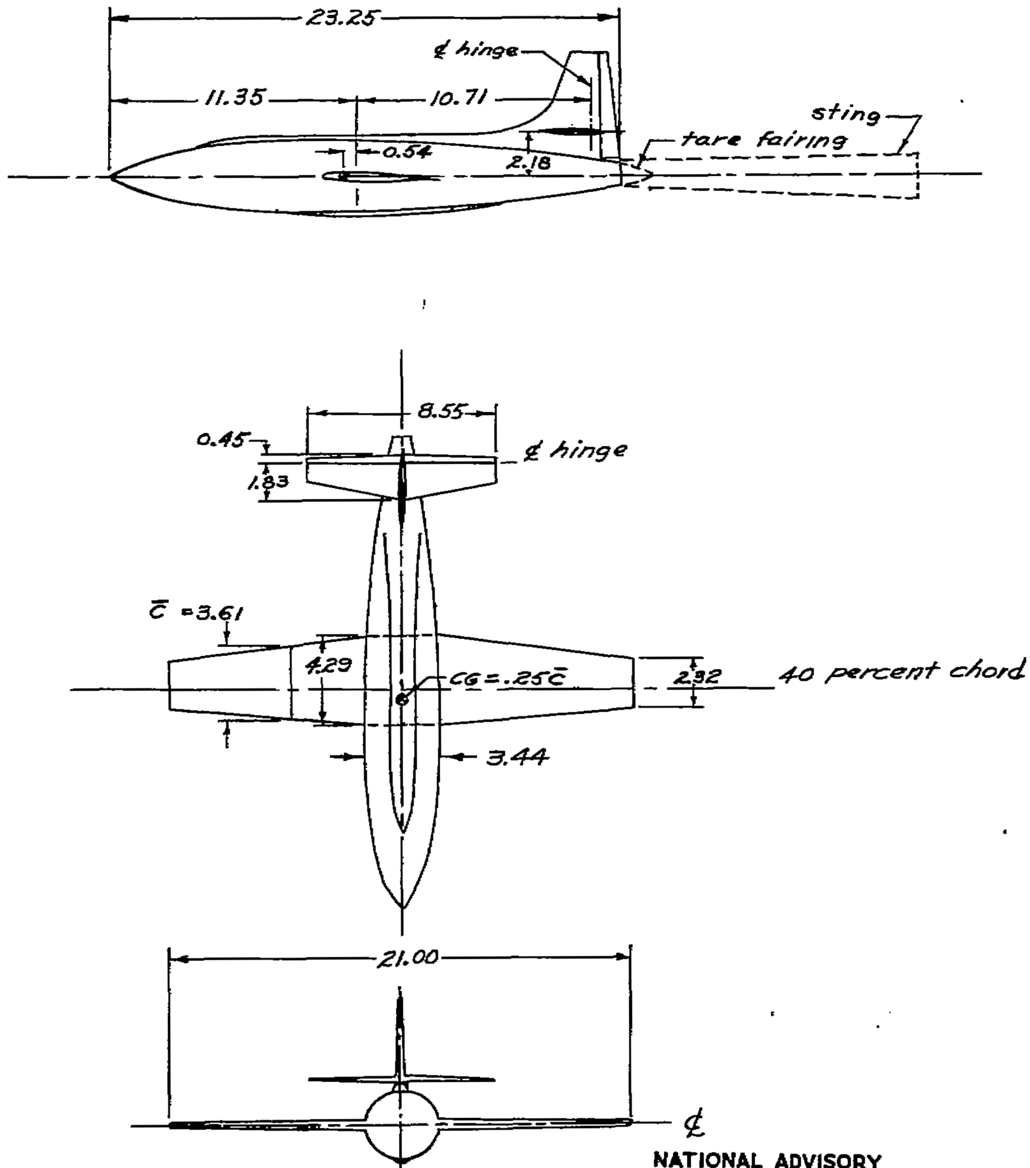

NATIONAL ADVISORY
COMMITTEE FOR AERONAUTICS

[redacted]

Figure 1.- Three view drawing of $\frac{1}{16}$-scale model of the Bell XS-1 airplane as tested in the Langley 8-foot high-speed tunnel. All dimensions in inches.

[redacted]

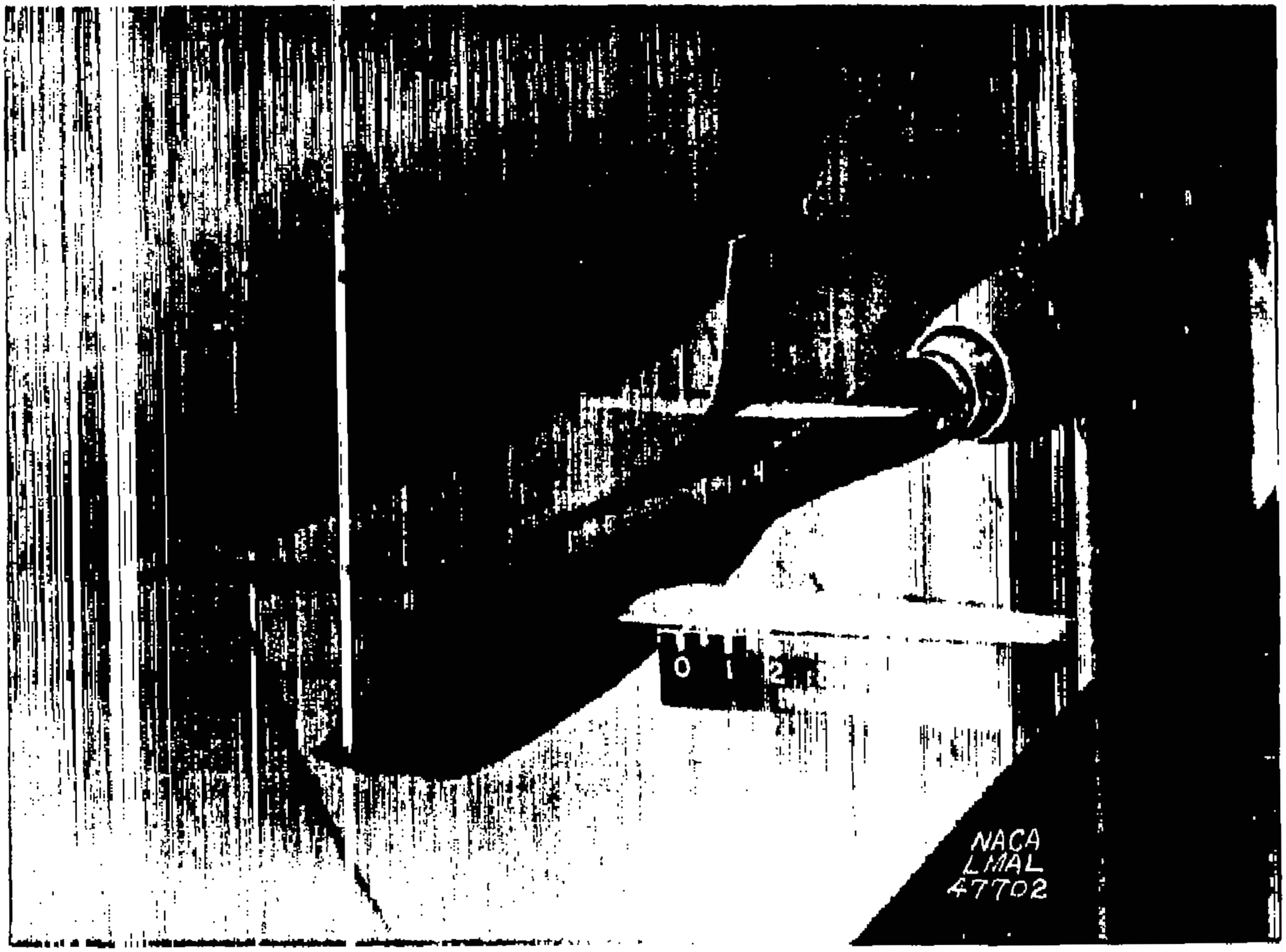

Figure 2.- $\frac{1}{16}$-scale model of XS-1 airplane mounted in the Langley 8-foot high-speed tunnel.

[redacted]

[redacted]

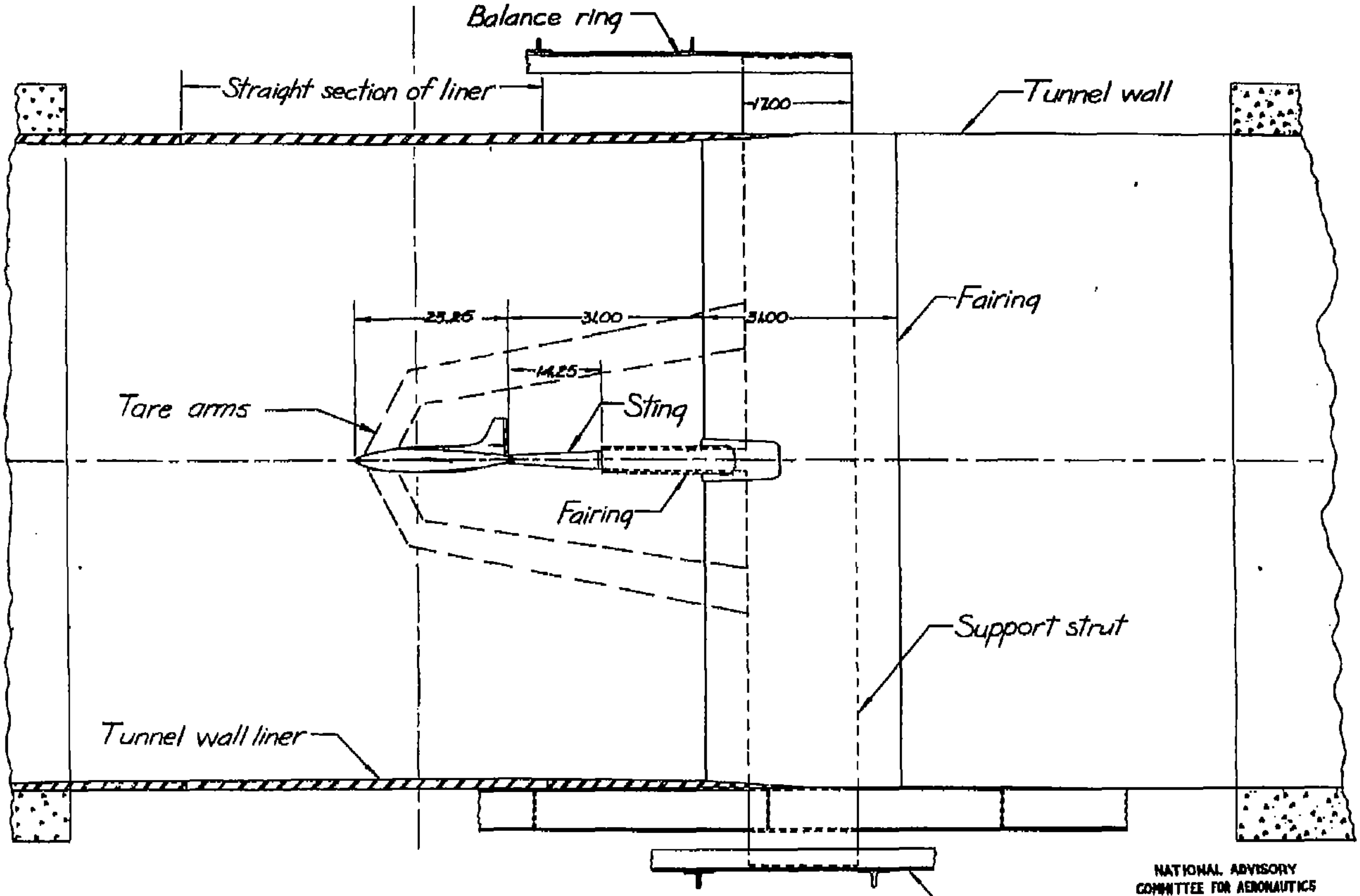

[redacted]

Figure 3.– XS-1 model on sting support in the Langley 8-foot high-speed tunnel.

[redacted]

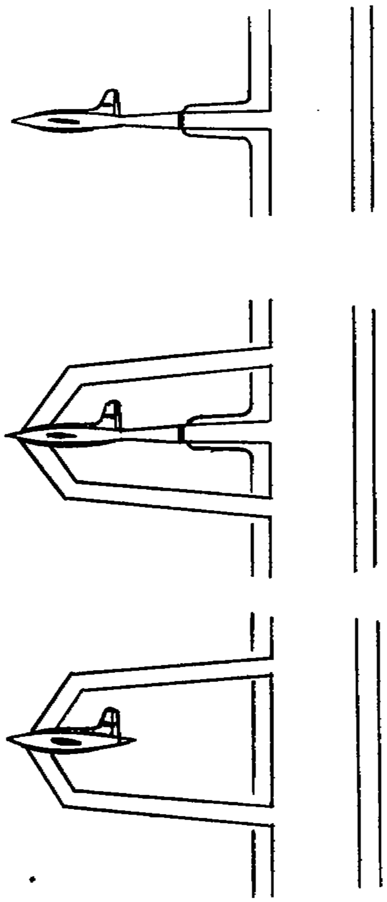

Balance Ring Measures

Normal Run

Model force
Sting force
Interference of sting on model
Interference of model on sting

Tare Run A

Model force
Sting force
Tare-arm force
Guy-wire force
Interference of model on arms
Interference of sting on model
Interference of model on sting
Interference of arms on model

Tare Run B

Model force
Tare-arm force
Guy-wire force
Interference of model on arms
Interference of arms on model

NATIONAL ADVISORY
COMMITTEE FOR AERONAUTICS

Tare Run A - Tare Run B	Sting force Interference of sting on model Interference of model on sting
Normal Run - (A - B)	Model force

Figure 4.- Tare setups and evaluation technique.

[redacted]

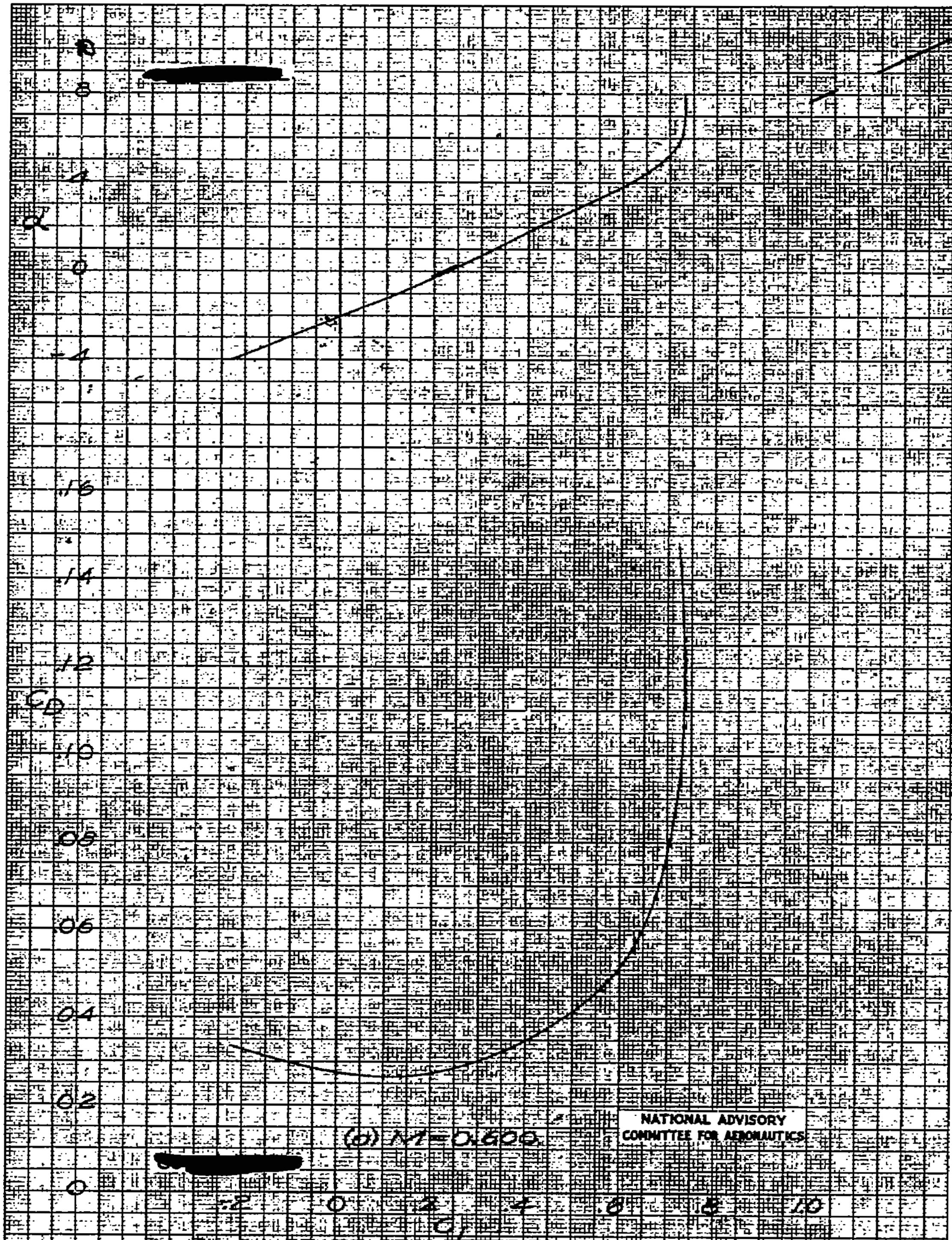

Figure 5.- Variation of drag coefficient and angle of attack with lift coefficient for complete model. $i_t = 0°$; $\delta_e = 0°$.

[redacted]

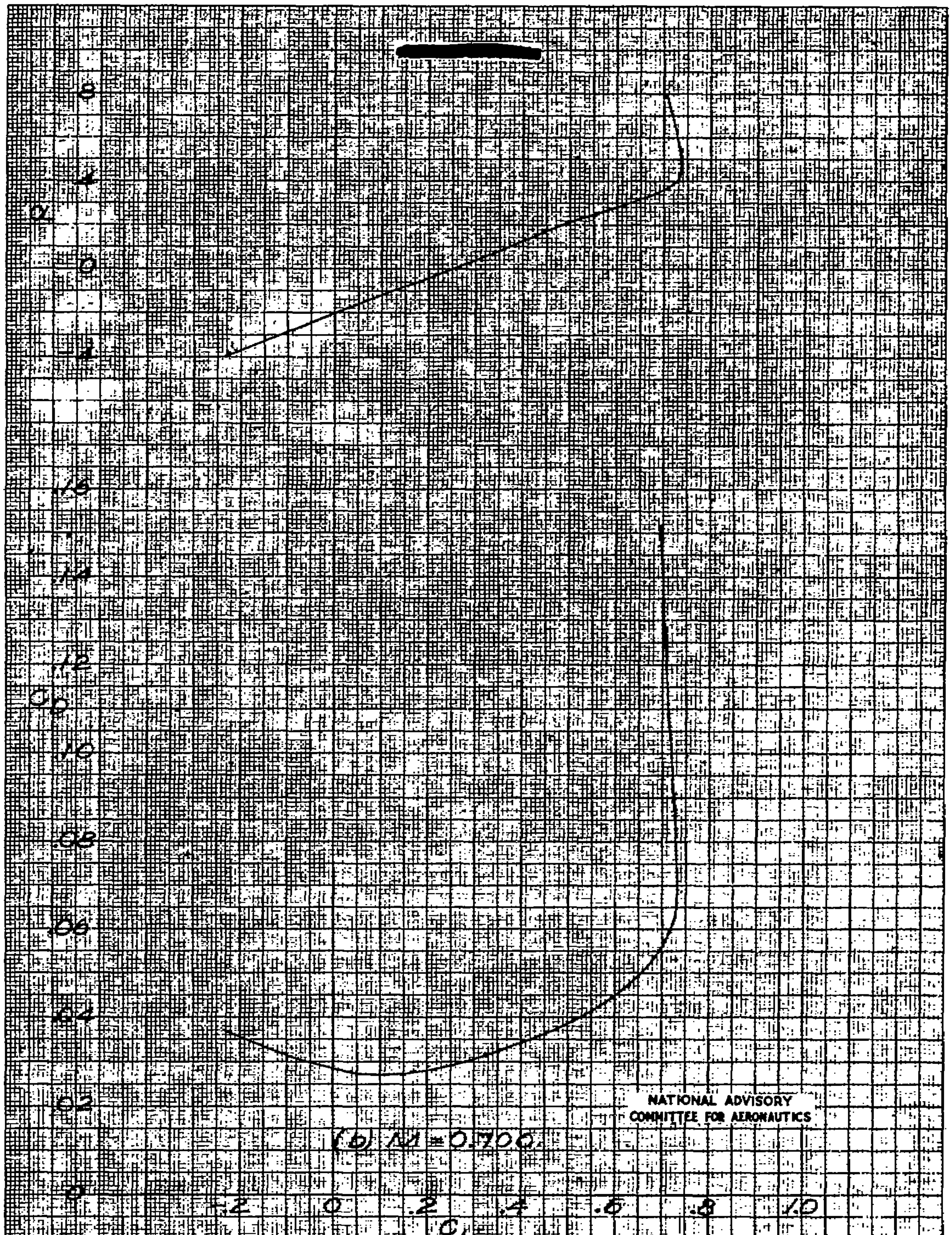

Figure 5.- Continued.

CO[redacted]

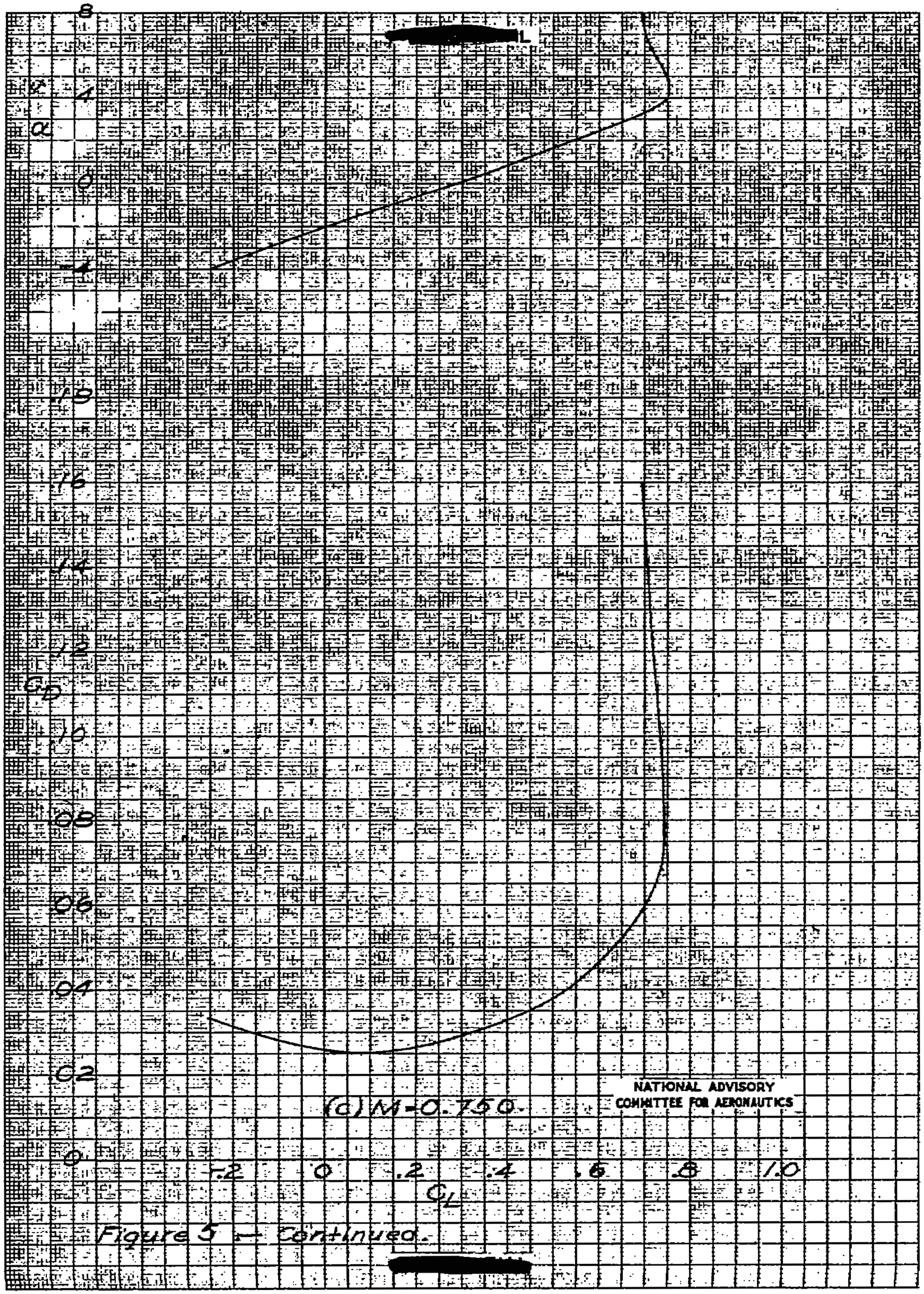

Figure 5 — Continued.

[redacted]

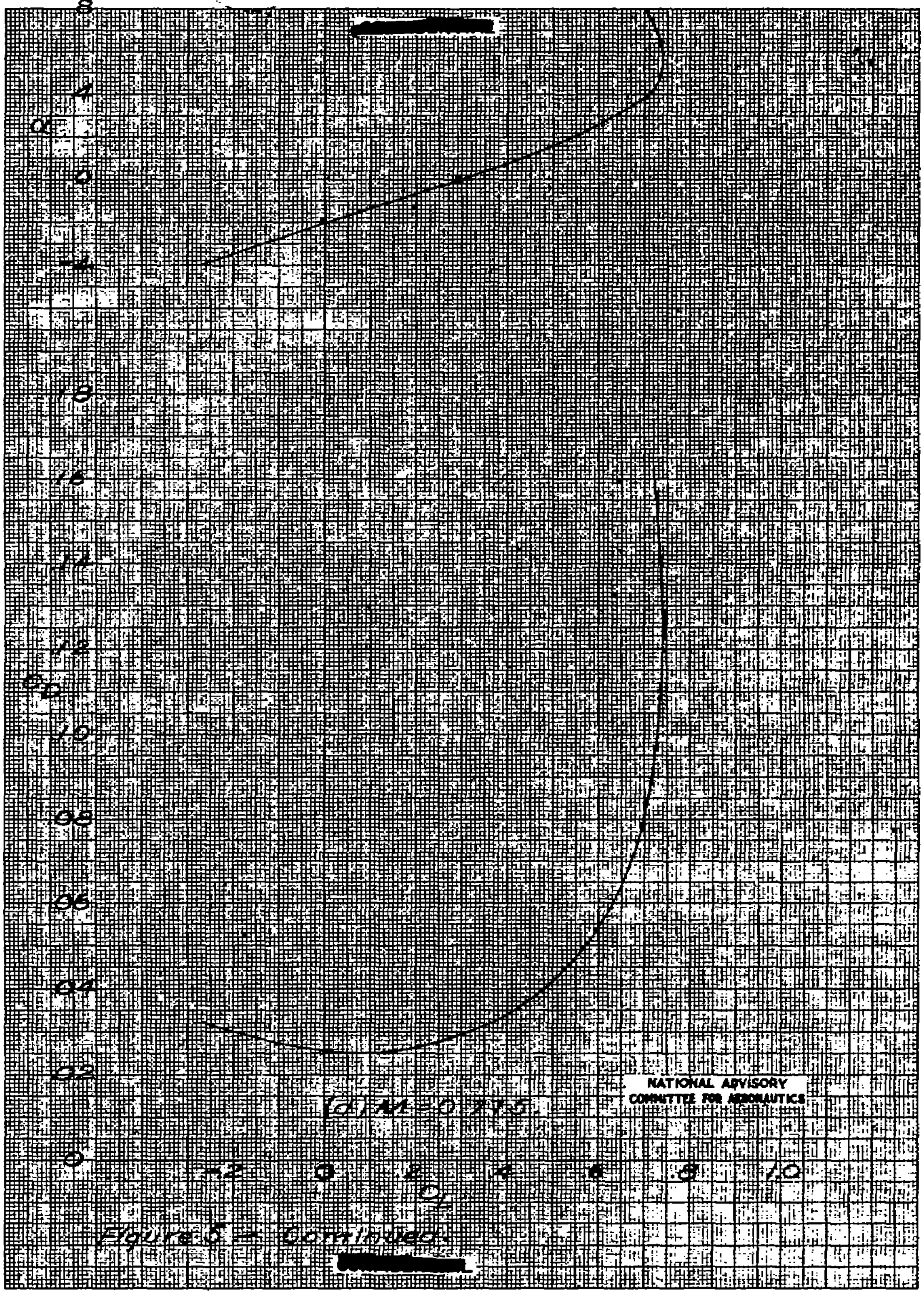

(d) M = 0.775.

Figure 5 – Continued.

[redacted]

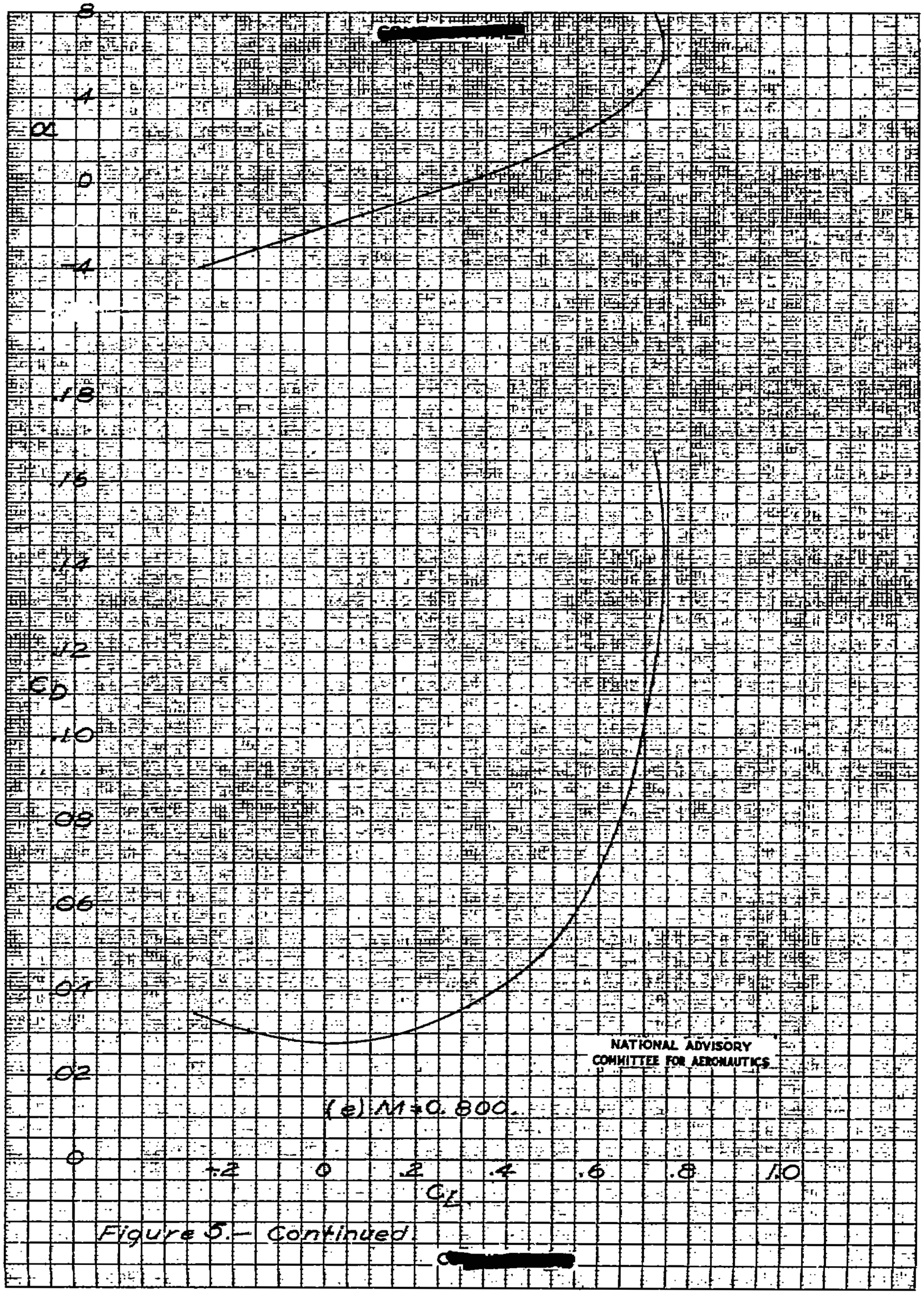

(e) M = 0.800.

Figure 5.– Continued.

[redacted]

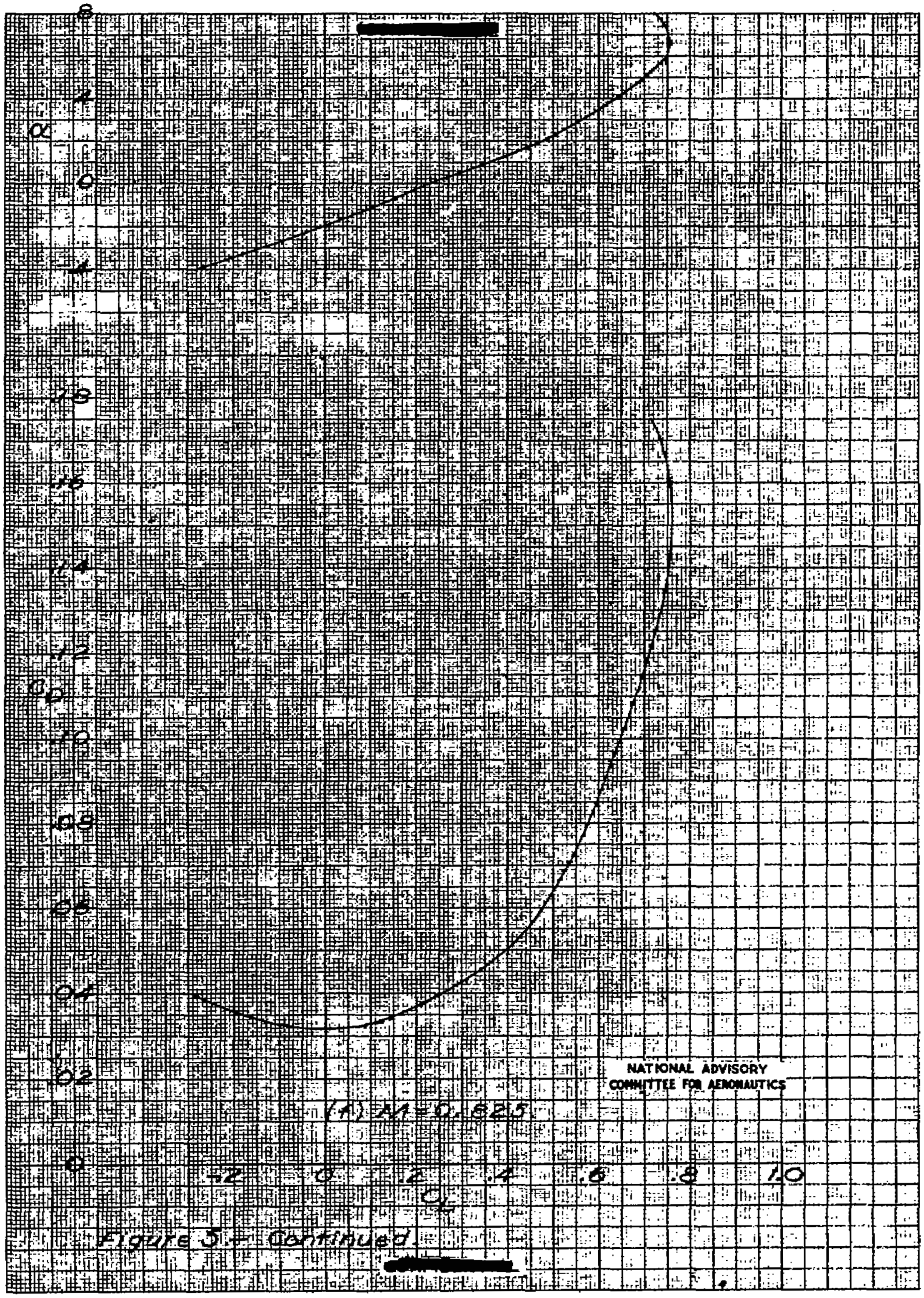

Figure 5.- Continued.

[redacted]

[redacted]

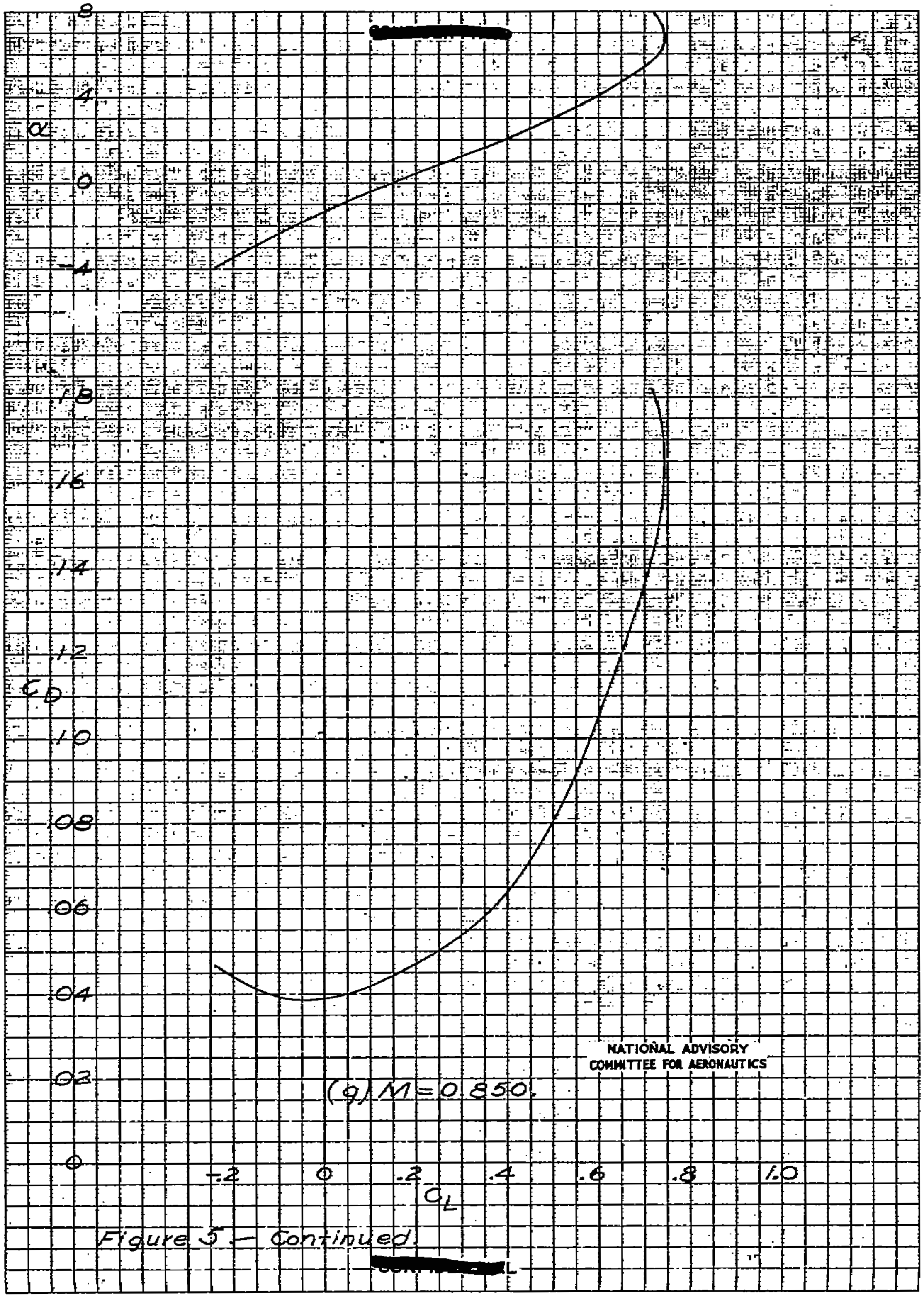

(g) M = 0.850.

Figure 5.— Continued.

[redacted]

[redacted]

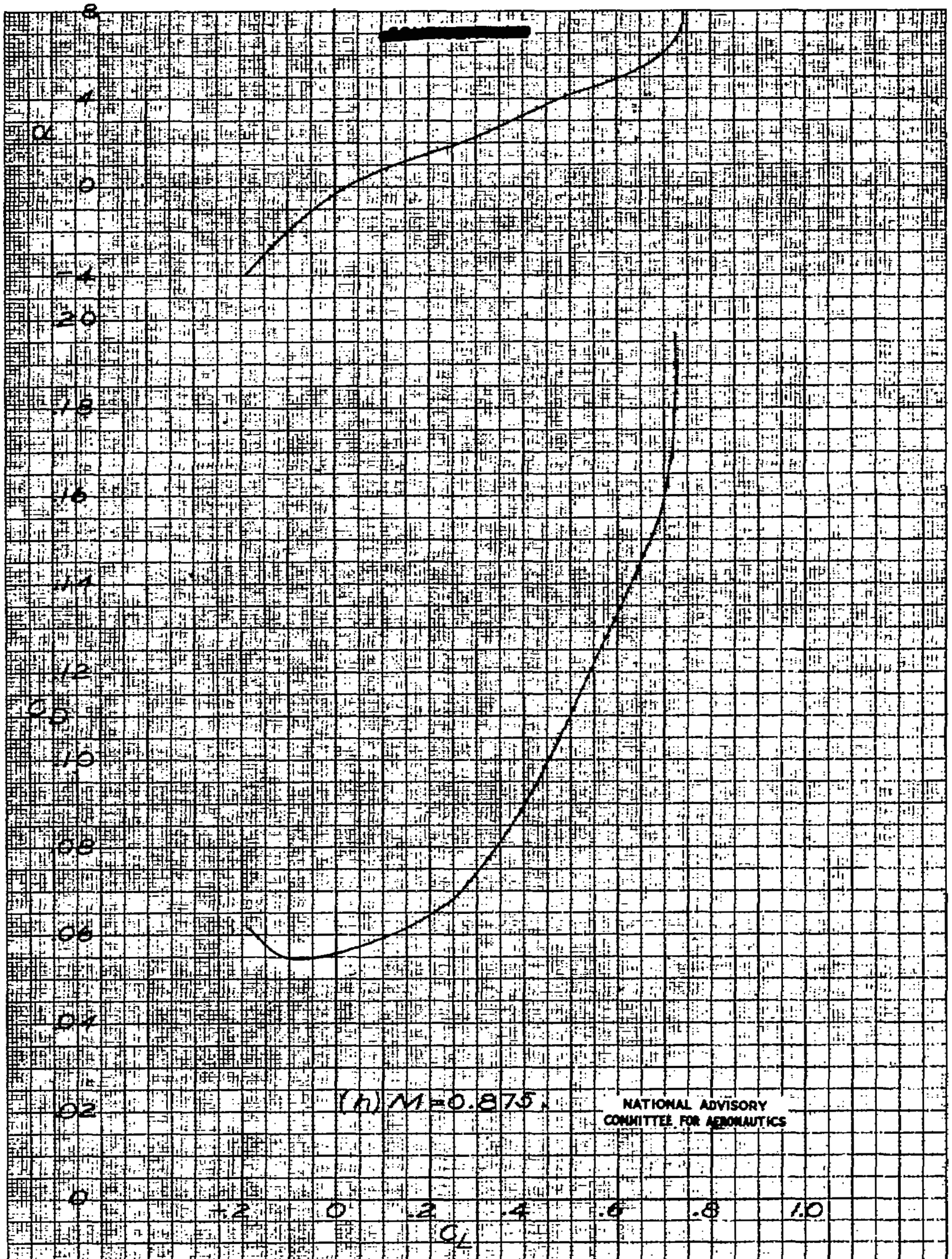

Figure 5 — Continued. [redacted]

[redacted]

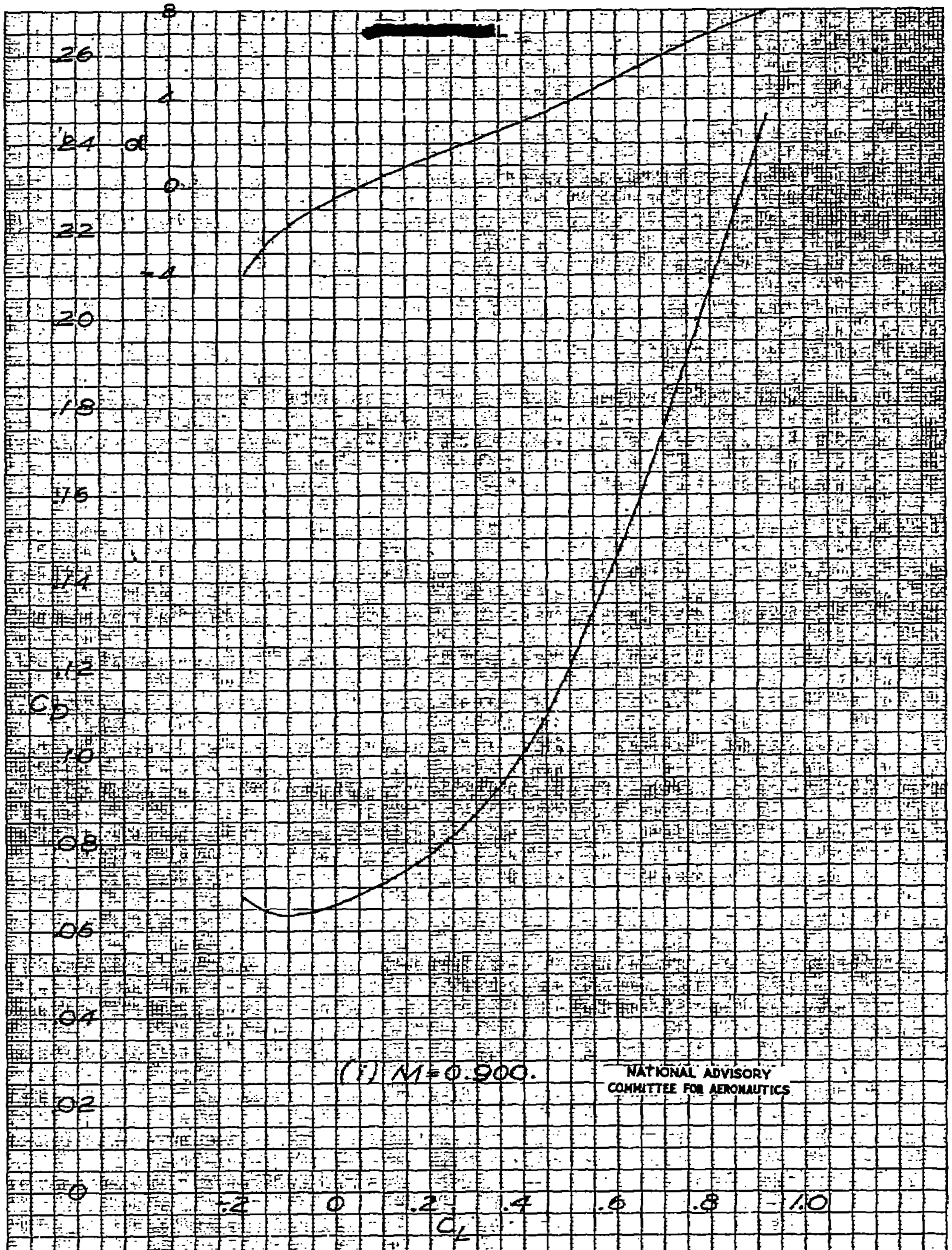

Figure 5 — Concluded.

[redacted]

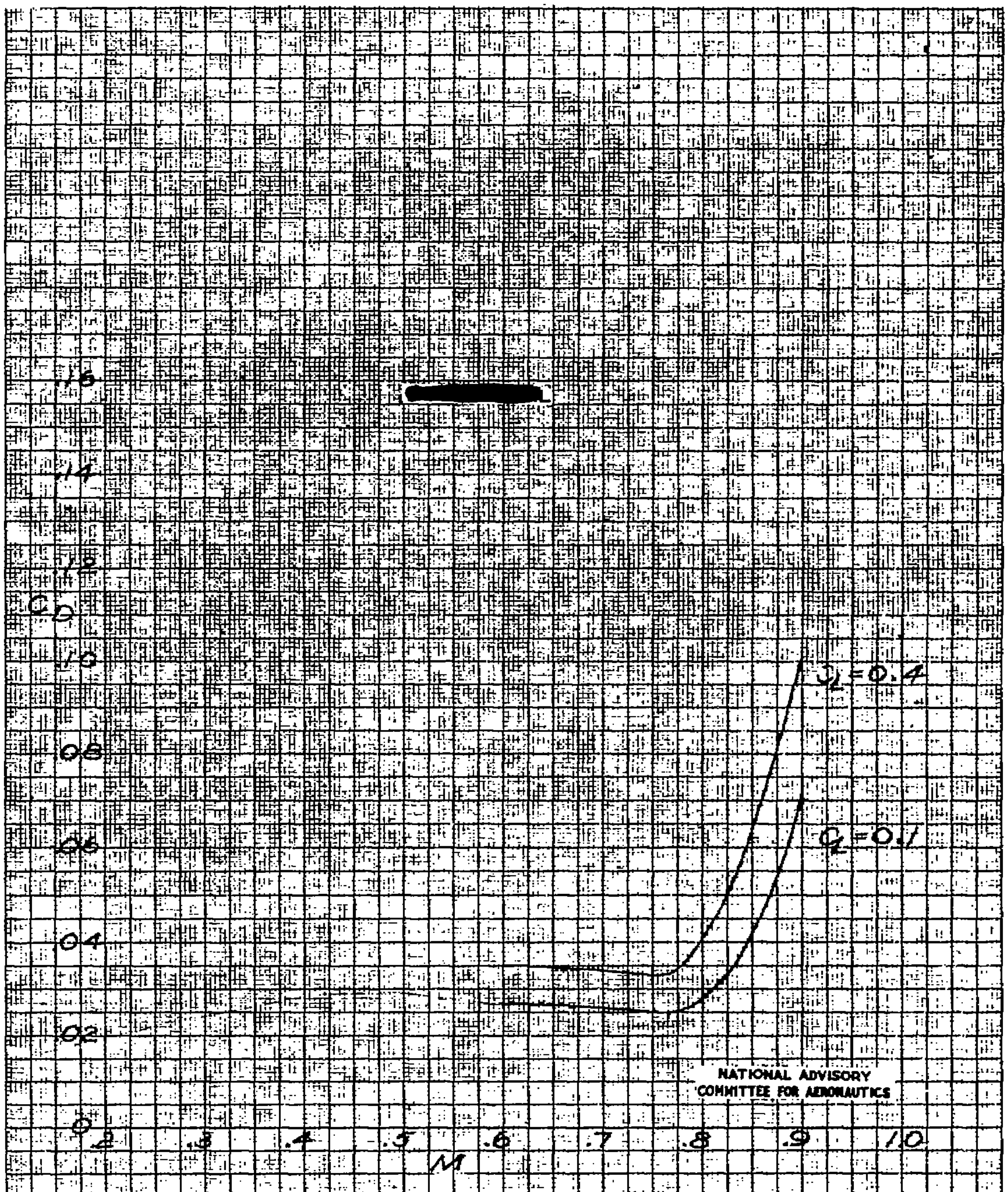

Figure 6.— Variation of drag coefficient with Mach number for complete model. $i_t=0°$; $\delta_e=0°$.

[redacted]

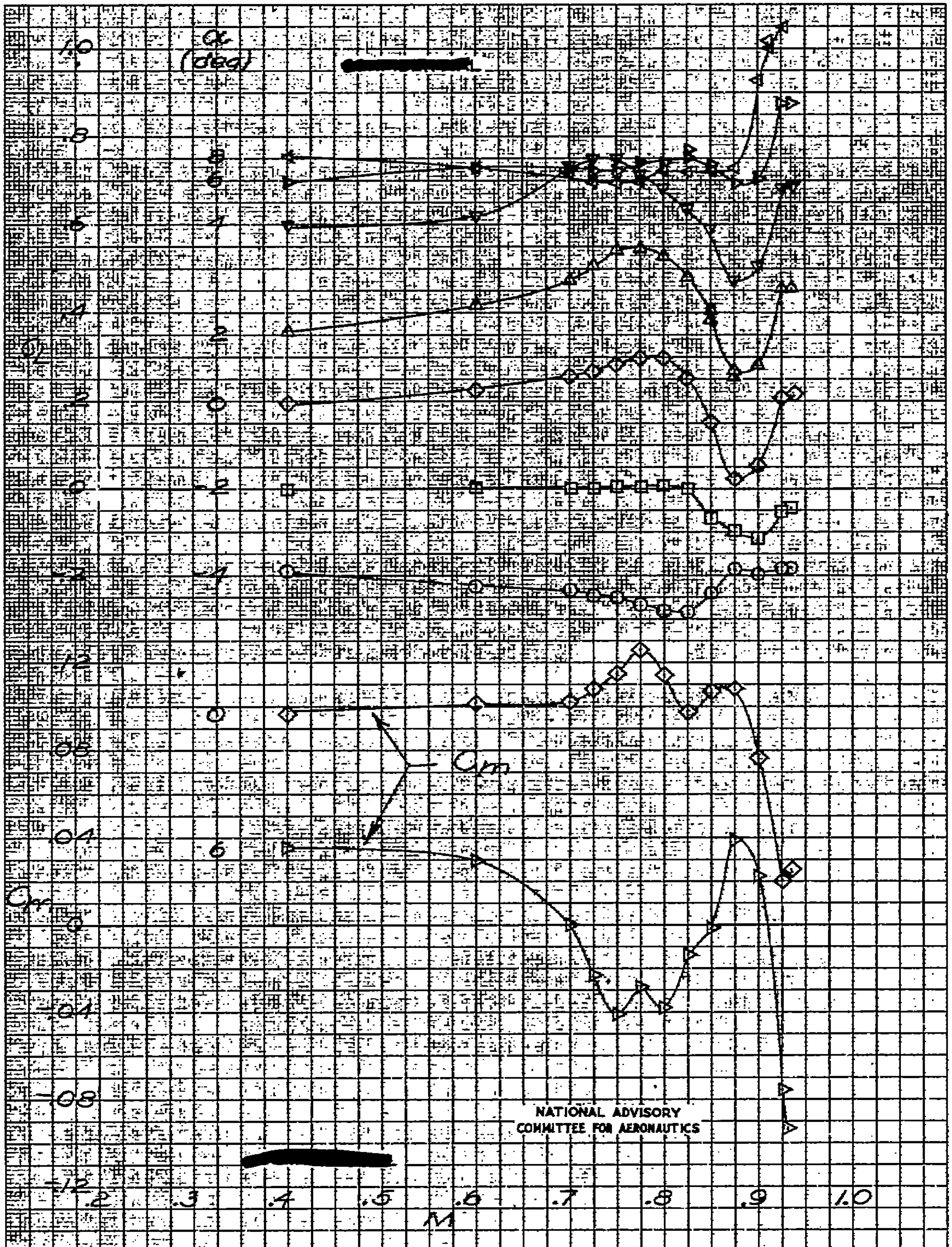

Figure 7.— Variation of lift coefficient and pitching-moment coefficient with Mach number for complete model. $i_t = 0°$; $\delta_e = 0°$

[redacted]

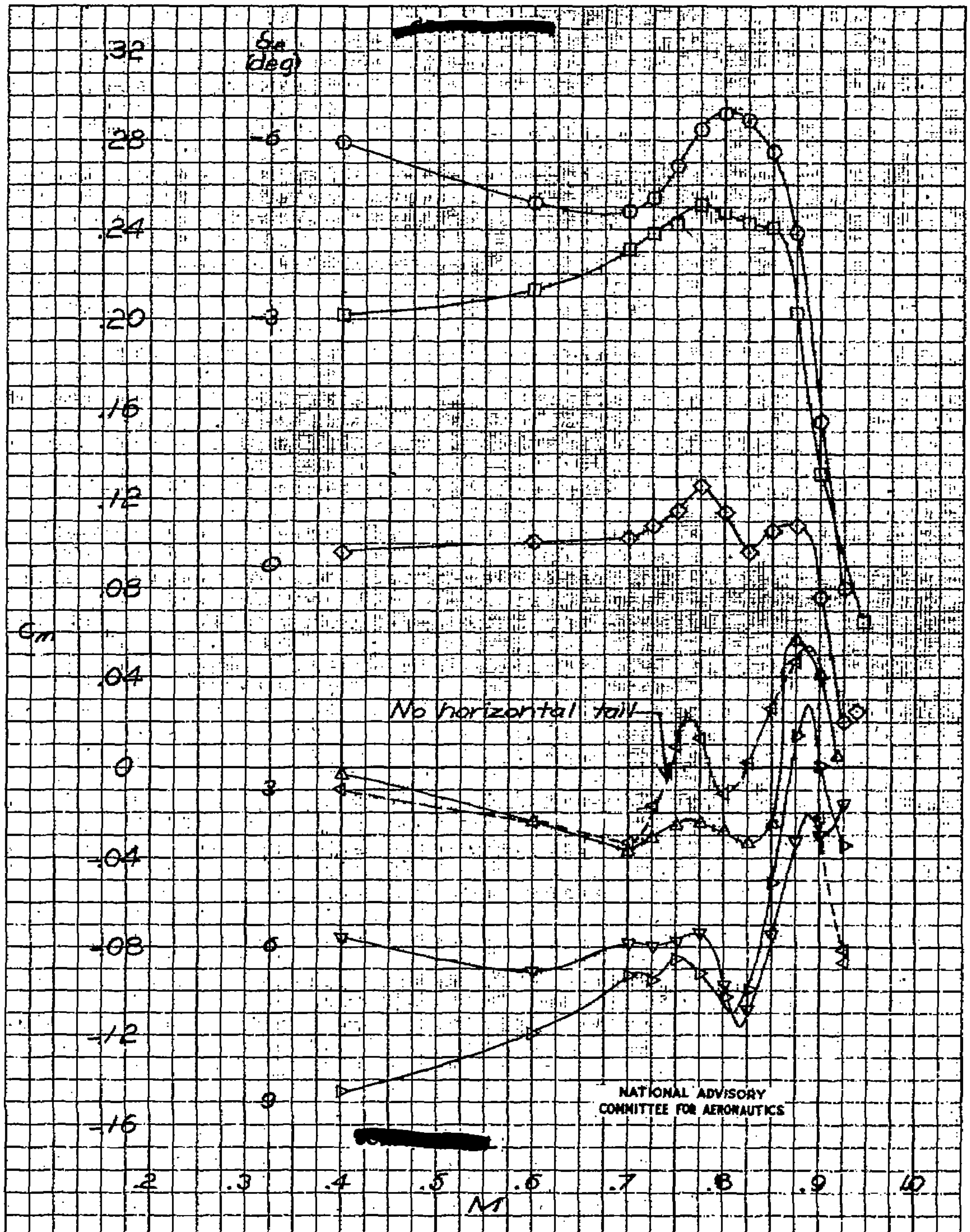

[redacted]

Figure 8.—Variation of pitching-moment coefficient with Mach number for various elevator deflections. $\alpha=0^\circ$; $i_t=0^\circ$.

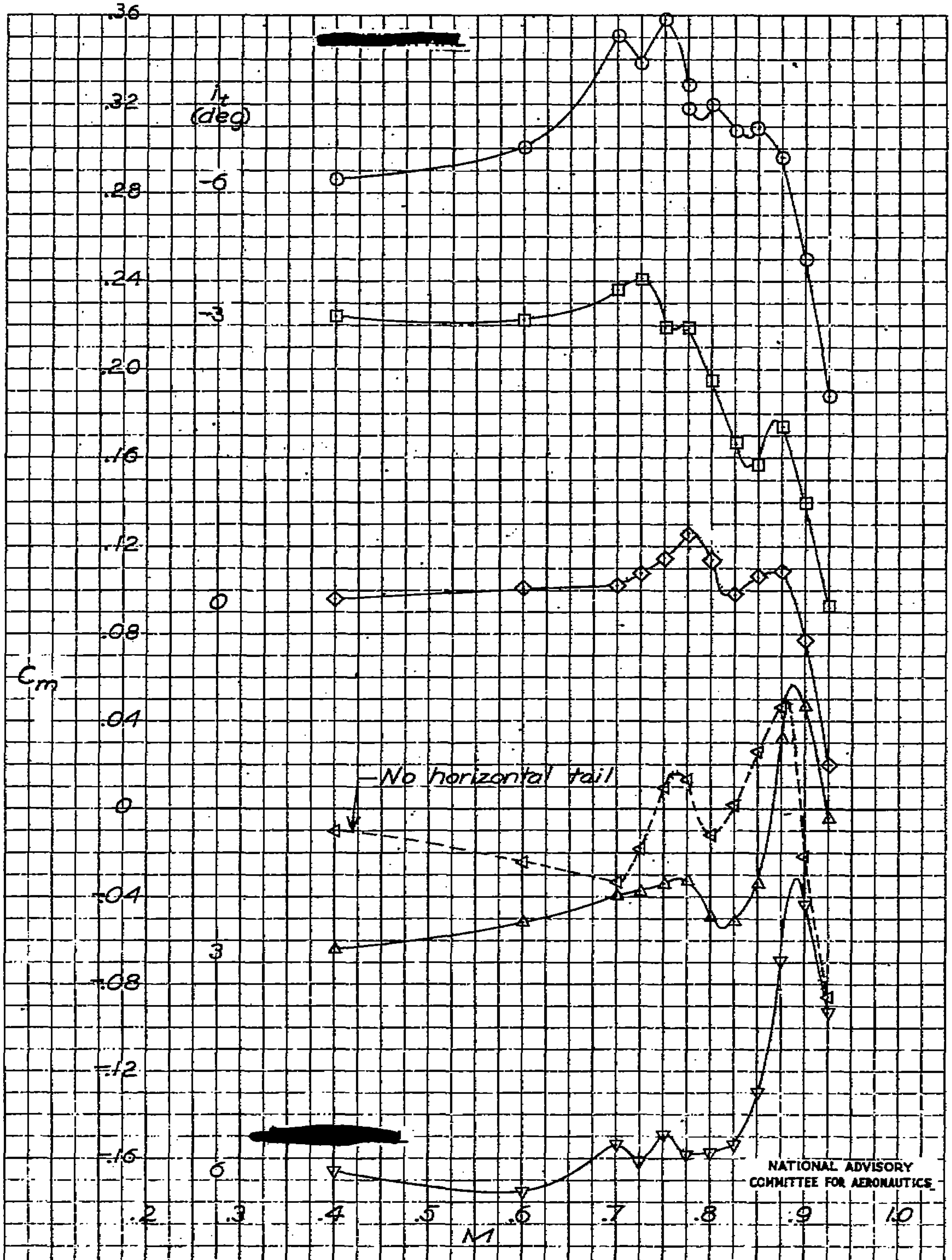

Figure 9. – Variation of pitching-moment coefficient with Mach number for various stabilizer angles. $\alpha = 0°$; $\delta_e = 0°$

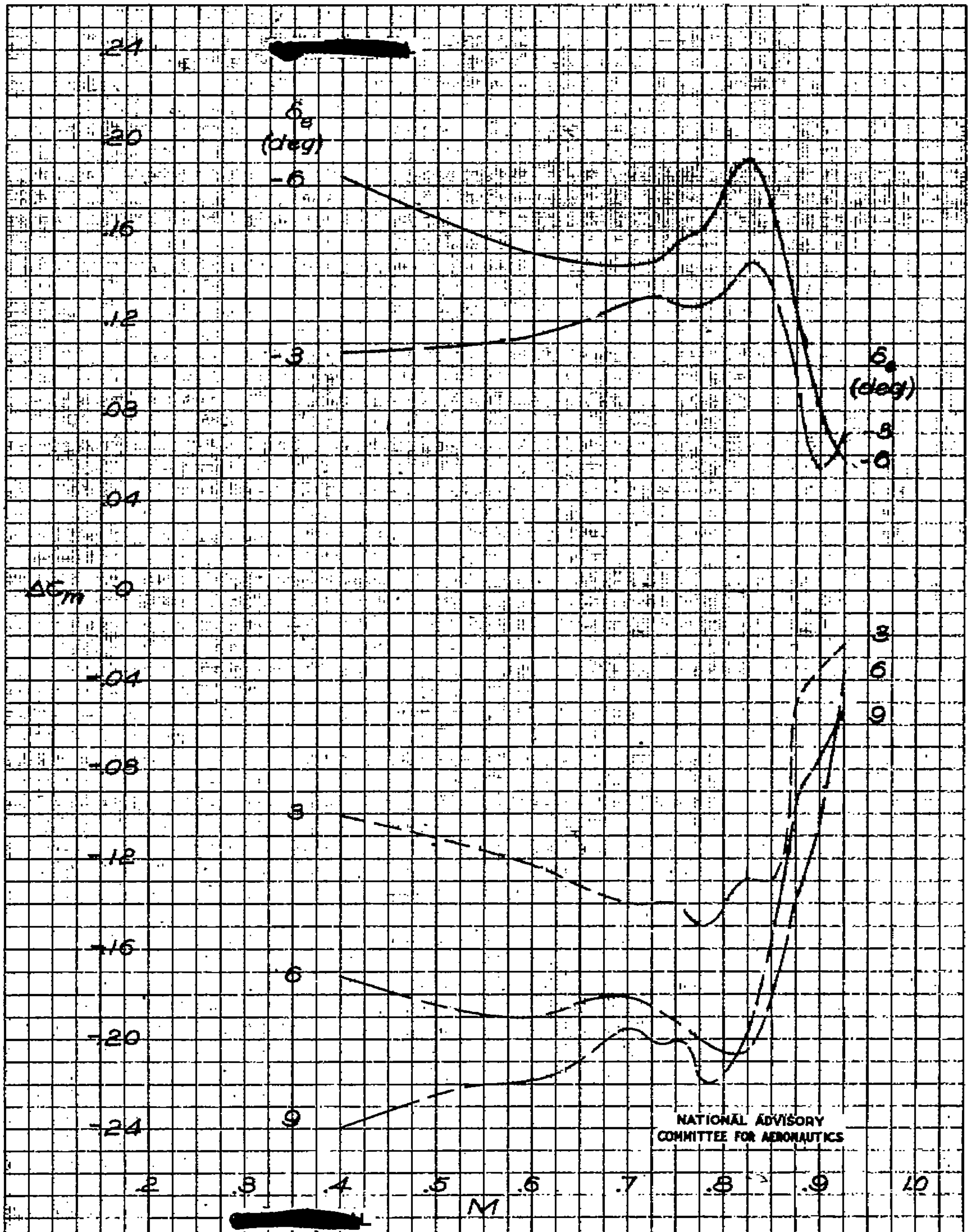

Figure 10.—Variation of elevator incremental pitching-moment coefficient with Mach number. $\alpha = 0°$; $i_t = 0°$.

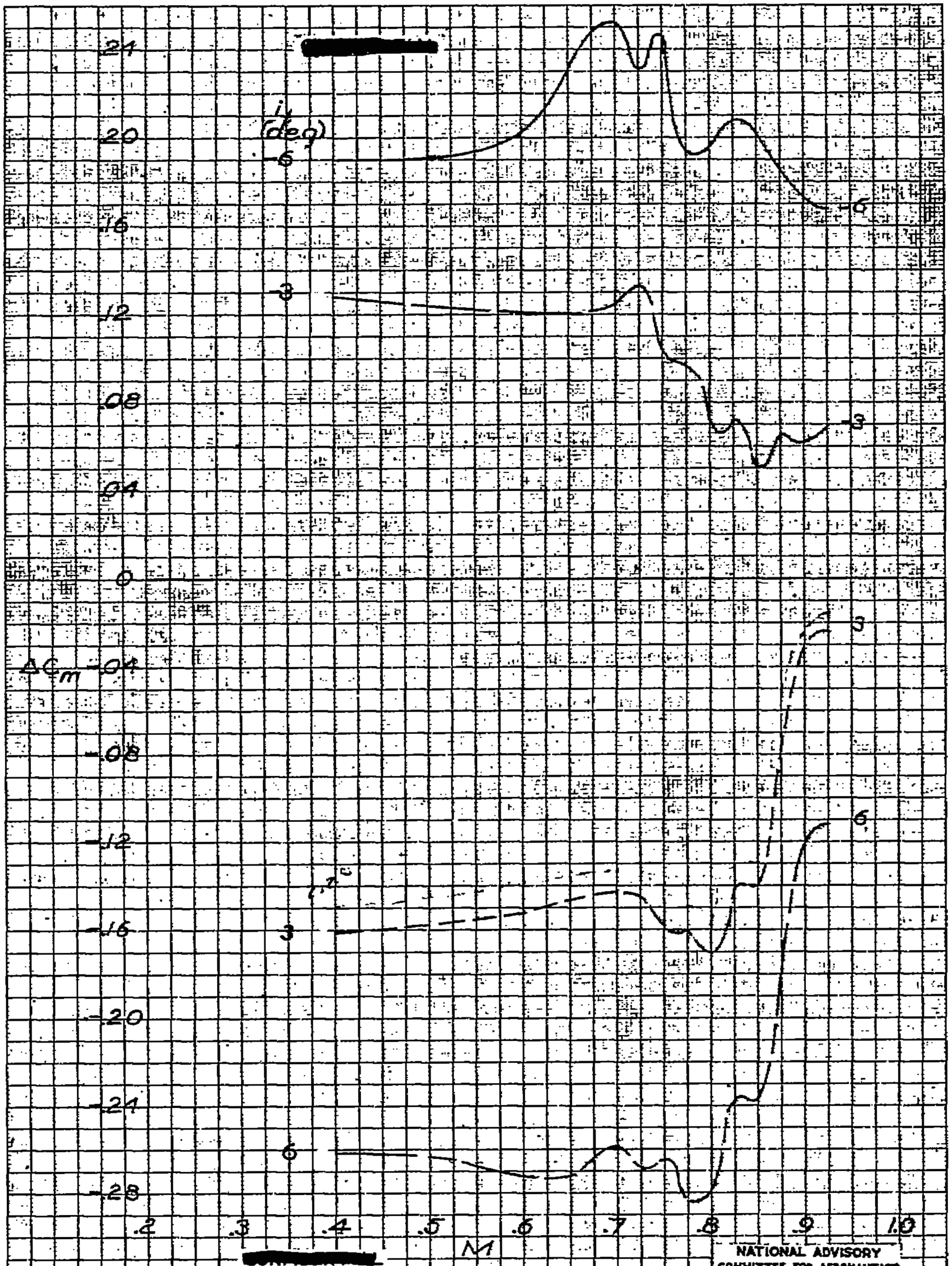

Figure 11.—Variation of stabilizer incremental pitching-moment coefficient with Mach number. $\alpha = 0°$; $\delta_e = 0°$.

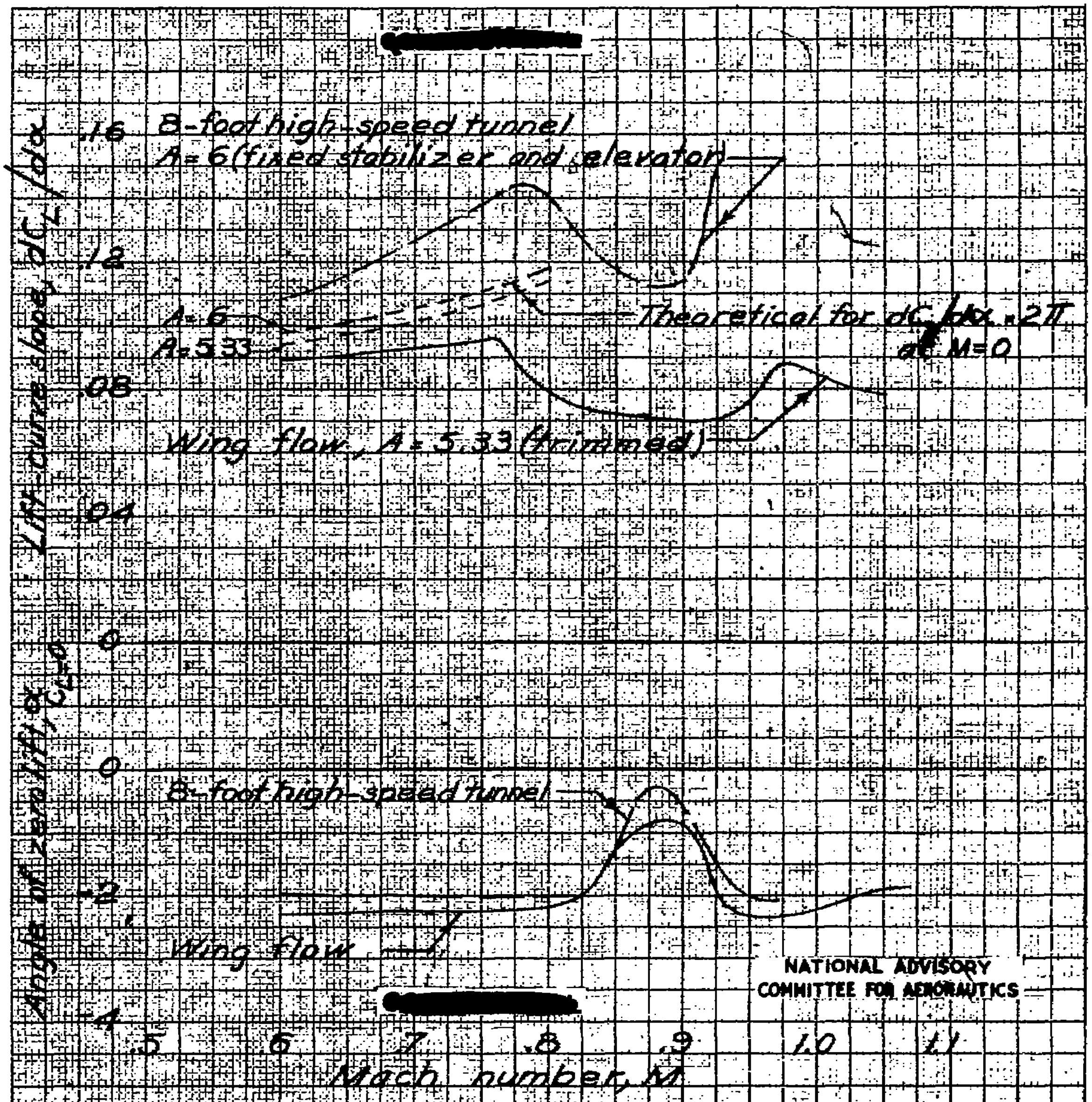

Figure 12.—Comparison of results of 8-foot high-speed tunnel tests of Bell XS-1 model and wing-flow tests of similar configuration.

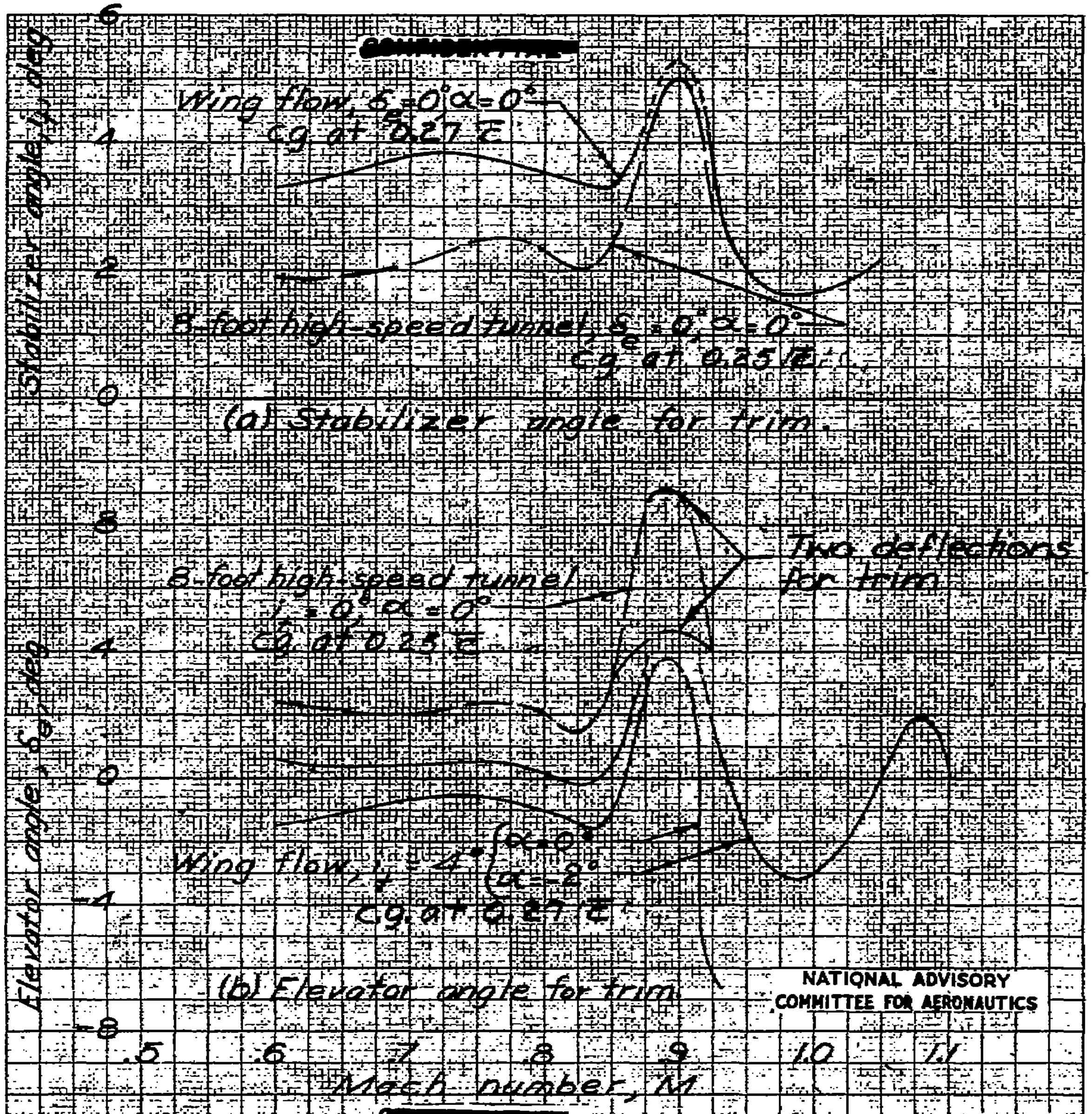

Figure 13.- Comparison of results of 8-foot high-speed tunnel tests of Bell XS-1 model, and wing-flow tests of similar configuration; variation with Mach number of stabilizer and elevator angles for trim at fixed angle of attack.